Network pharmacology and molecular docking analysis on molecular targets and mechanisms of *Gastrodia elata* Blume in the treatment of ischemic stroke

YUAN LUO, PU CHEN, LIPING YANG and XIAOHUA DUAN

Yunnan Key Laboratory of Dai and Yi Medicines, Yunnan University of Chinese Medicine, Kunming, Yunnan 650500, P.R. China

Received April 21, 2022; Accepted September 13, 2022

DOI: 10.3892/etm.2022.11678

Abstract. *Gastrodia elata* Blume (GEB) is widely used to treat cardio-cerebrovascular disease in China and in traditional Chinese medicine it is considered to be a dispelling wind and dredging collateral. However, the mechanism and active components of the plant in treating ischemic stroke (IS) remain unclear. The present study aimed to identify the active components and mechanism of GEB in treating IS using network pharmacology and molecular docking technology. Network analysis predicted 752 potential targets from 14 compounds in GEB, sharing 32 key targets with IS-associated targets. Gene Ontology analysis of key targets showed that 'oxidative stress', 'immune response' and 'regulation of blood circulation' were significantly enriched. Kyoto Encyclopedia of Genes and Genomes pathway analysis indicated that the key targets regulated 11 representative pathways including 'arachidonic acid metabolism', 'lipid and galactose metabolism'. In the protein-protein interaction network, five core targets, including toll-like receptor agonist, STAT3, myeloperoxidase (MPO), prostaglandin-endoperoxide synthase and matrix metalloproteinase (MMP)9, were identified and successfully docked with four active components: Palmitic acid, alexandrin, para-hydroxybenzaldehyde and gastrodin. Alexandrin, para-hydroxybenzaldehyde, and gastrodin are closely related to brain ischemia/reperfusion damage and repair. Therefore, to further verify the mechanism of action of three active components in the second part, we established the HT22 oxygen-glucose deprivation-reperfusion (OGD/R) model. Cell Counting Kit-8 assay and western blot analysis demonstrated that these three active components of GEB regulated core targets of molecular docking, such as STAT3, MPO and MMP9. *In vitro* experiments showed that OGD/R decreased cell survival, while this effect was reversed by the three active components of GEB. In addition, western blot analysis indicated that alexandrin upregulated expression of phosphorylated-STAT3, para-hydroxybenzaldehyde downregulated MPO and gastrodin downregulated MMP9. Therefore, the present study showed that GEB may prevent and treat IS via interaction between the active components and the main targets, which is key for investigating the efficacy of traditional Chinese medicine.

Introduction

Stroke is the leading cause of disability and the second leading cause of death globally (1). Ischemic stroke (IS) accounts for ~80% of stroke cases and has become a major public health concern in the 21st century (2). At present, although clinical drugs and mechanical thrombolytic therapy have made progress in patient recovery (3), due to the time constraints of reperfusion therapy (to be administered within 4.5-6 h of stroke), secondary brain injury increases the risk of disability and recurrence of stroke in patients (4). Therefore, early prevention and treatment of IS are key challenges and need further investigation.

The lack of specific medicines against IS has led to emergence of alternative and complementary therapy (5). For example, the World Health Organization (WHO) recommends acupuncture as an alternative and complementary strategy for stroke treatment (6). Chinese herbal medicines, such as Mailuoning, Xuesaitong, and BuchangNaoxintong were the patented Chinese herbal medicines likely to improve stroke recovery and have shown potential in complementary and alternative interventions for stroke treatment (7,8). In traditional Chinese medicine (TCM), it is considered that *Gastrodia elata* Blume (GEB) contrasts hyperactive liver, dispels wind and dredges collaterals (9). Moreover, GEB has been used as an anticonvulsant in Asian countries for several centuries (10). Specifically, several classical formulations of GEB have been widely used in clinical practice, such as Tianma Gouteng and Banxia Baizhu Tianma decoction for treating

Correspondence to: Dr Xiaohua Duan, Yunnan Key Laboratory of Dai and Yi Medicines, Yunnan University of Chinese Medicine, 1076 Yuhua Road, Chenggong, Kunming, Yunnan 650500, P.R. China
E-mail: duanxiaohua@ynutcm.edu.cn

Key words: Gastrodia elata blume, ischemic stroke, network pharmacology analysis, molecular docking, pharmacological mechanism

stroke, dementia and other neurodegenerative disease (11,12). In addition, GEB Chinese patent medicine is frequently used in the clinic. For example, Tianma injection in 53 patients with vertebrobasilar insufficiency showed a total effective rate significantly higher than that in the control group (13). Moreover, Tianma Duzhong capsule prescribed for the treatment of acute cerebral infarctions in 36 patients exhibited an effective rate of ~90% based on European Stroke Score (14). In a previous study, ethyl acetate extract of GEB showed a protective effect on ischemia/reperfusion (I/R) in rats by preventing death of hippocampal CA1 cells and significantly decreasing disruption of the blood-brain barrier (BBB) (15,16). In addition, both *in vitro* and *in vivo* studies have shown that GEB and its compounds protect against IS by decreasing damage to the neurological function and improving the energy metabolism of mitochondria (11,17). However, the treatment methods commonly used in clinical practice have limitations, such as poor brain targeting and limited ability to cross the BBB (18). Also, the mechanism and efficacy of GEB in preventing IS remain unclear. Therefore, it is essential to explore the effects of the GEB components and their targets in IS.

Network pharmacology analysis has revealed that the drug-gene-target-disease interaction underlies the pharmacodynamic mechanism of the main components and targets (19). Moreover, this is consistent with the holistic view of TCM and the compatibility of TCM syndrome differentiation (20). In the current study, differentially expressed genes (DEGs) were screened using the Gene Expression Omnibus (GEO) database. Gene Ontology (GO) and Kyoto Encyclopedia of Genes and Genomes (KEGG) enrichment analyses were used to study the roles of target genes in cells and signaling pathways. Finally, molecular docking and western blotting were used to demonstrate the association between key target genes and GEB molecular components. The workflow of network pharmacology is shown in Fig. 1. Thus, the present study aimed to elucidate the mechanism by which GEB treats IS and its implications for exploring new clinical approaches.

Materials and methods

Active ingredient analysis. GEB was used as a keyword to retrieve its active ingredient using the encyclopedia of TCM (ETCM; tcmip.cn/ETCM/index.php/Home/Index/) and systematically review the chemical structure of active ingredients in the TCM system pharmacology database and analysis platform (TCMSP; https://tcmsp-e.com/). The detailed screening process is shown in Fig. S1.

Multiple database mining of active ingredient target and disease-associated genes. Target genes for the major active compounds in GEB were mined using the ETCM and SwissTargetPrediction (swisstargetprediction.ch/) databases. A merge-and-de-duplicate analysis produced a list of the final compound target genes. SwissTargetPrediction database predicted the target based on two- and three-dimensional (3D) similarity analysis of known ligands (21).

Disease-associated genes were accessed through five databases: GeneCards (genecards.org), Gene-Disease Networks (DisGeNet) (disgenet.org), DrugBank (drugbank.ca), Online Mendelian Inheritance in Man (OMIM) (ncbi.nlm.nih.gov/omim) and Therapeutic Target Database (TTD) (system-sdock.unit.osit.jp/iddp/home/index). The disease-associated genes were collected using IS as a keyword and merge-de-duplication analysis.

Identification of disease-associated DEGs. GSE16561 dataset (ncbi.nlm.nih.gov/geo/query/acc.cgi?acc=GSE16561) containing peripheral whole-blood RNA sequencing data from 39 patients with IS and 24 healthy control subjects was downloaded from the GEO database. Subsequently, differential expression analysis was performed using R package limma (version 3.44.3) (22) with IS vs. healthy subjects to identify DEGs associated with IS. $|Log_2$fold-change (FC)$|>0.5$ and $P<0.05$ were used to determine differential expression.

Functional annotation. Functional enrichment analysis focused on key genes. The overlap of compound target and potential disease-associated genes with IS-associated DEGs were defined as key genes for treatment of IS using GEB. R package clusterProfiler (version 3.18.0) (23) used for the enrichment analysis of key genes was applied to GO and KEGG. GO contains three main categories, biological processes (BP), cellular components (CC) and molecular functions (MF). Adjusted $P<0.05$ indicated significantly enriched entries.

Network of effective active ingredients and key genes. The potentially active compounds and key genes of GEB and IS were entered into Cytoscape software (version 3.2.1) (24) to develop the herb-compound-targets-disease network, where nodes represented potentially active compounds of GEB and the key targets of IS. The edges (linear segments) showed association between these factors.

Protein-protein interaction (PPI) network construction and degree value analysis. STRING (version 11.0) (25) database was used to analyze interactions between the key genes previously identified for GEB treatment of IS (confidence score, 0.4) (26). Cytoscape (version 3.2.1) (24) was used to generate a PPI network map. In addition, the CytoNCA plugin (version 2.1.6) (27) in Cytoscape was used to analyze the connectivity of proteins in the PPI network (27). The results were sorted by degree and the top five genes were identified as core candidates for subsequent analysis.

Molecular docking. Molecular docking was performed using AutoDock Vina (version 1.1.2) (28) and PyMOL (version 2.4.1) (29) to confirm the binding activity of the core components of GEB to potential targets. The binding activity is expressed as binding energy. The lower the binding energy, the more stable the docking module (30,31). In general, docking energy <-4.25 kcal/mol has docking activity, docking energy <-5 kcal/mol has good docking activity, while docking energy <-7 kcal/mol has very strong docking activity (32). Briefly, protein crystal structures of key genes were first obtained from the Protein Data Bank (rcsb.org/), where water and other small molecules were removed using PyMOL and hydrogen atoms and charge manipulations were added using AutoDock. Moreover, the 3D structures of core compounds were downloaded from the PubChem database (pubchem.ncbi.nlm.nih.gov/) and imported into AutoDock to add charge and

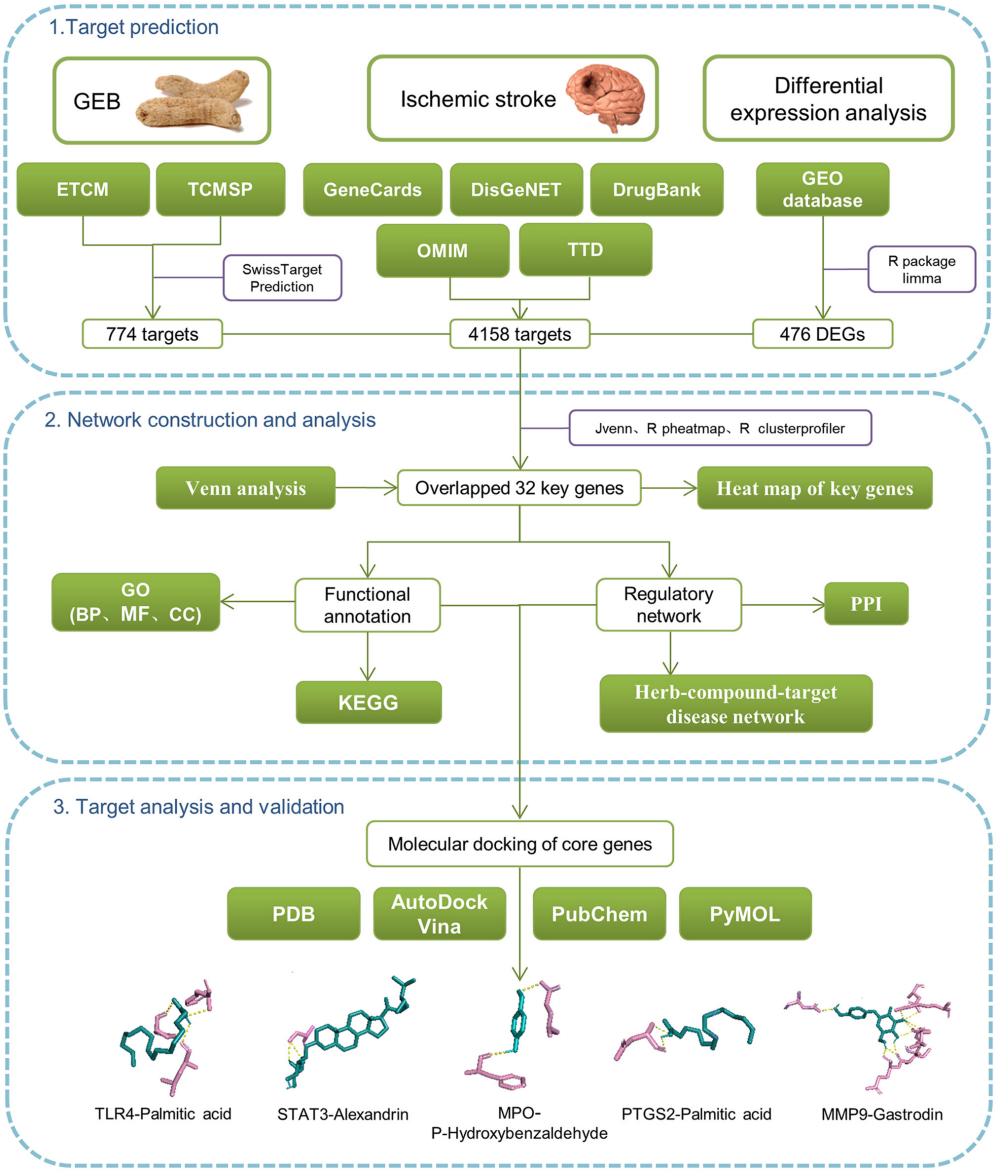

Figure 1. Flowchart of network pharmacology and molecular docking. ETCM, encyclopedia of traditional Chinese medicine; GEB, *Gastrodia elata* Blume; TCMSP, The traditional Chinese medicine systems pharmacology database and analysis platform; DEG, differentially expressed gene; PPI, protein-protein interaction; KEGG, Kyoto Encyclopedia of Genes and Genomes; GO, Gene Ontology; BP, biological processes; MF, molecular functions; CC, cellular components; PDB, protein databank; TRL4, toll-like receptor 4; MPO, myeloperoxidase; PTGS2, prostaglandin-endoperoxide synthase.

display the rotatable bonds. The core compounds were used as ligands and proteins corresponding to the core genes were used as receptors for molecular docking. Subsequently, the binding affinity between these core compounds and the core proteins was used as the evaluation criteria. The structure with the lowest docking energy (the highest binding affinity) in the output results was selected. PyMOL was used to visualize the combination of the best docking scores.

Statistical analysis. All statistical analysis was performed using R software (version 4.0.3). Volcano maps were plotted using R package ggplot2 (version 3.3.2) (33) to visualize the distribution of DEGs. The expression heat map of key genes in the GSE16561 dataset was generated using the R package Pheatmap (version 0.7.7) (34). The bubble and chord plots showing the functional enrichment results were visualized using the R package GOplot (version 1.0.2) (35). The thresholds representing the statistical significance were $|\log_2$fold-change (FC)$|>0.5$ and $P<0.05$.

Experimental verification

Materials. Para-hydroxybenzaldehyde, gastrodin and alexandrin were purchased from Chengdu Alfa Biotechnology Co., Ltd. (purity, ≥98%). Sodium dithionite ($Na_2S_2O_4$) was purchased from Shanghai Macklin Biochemical Co., Ltd. HT22 cells were obtained from Shanghai Biological Technology Co., Ltd. Primary antibodies against phosphorylated (p)-STAT3 (cat. no. AF3293), STAT3 (cat. no. AF6294) and matrix metalloproteinase (MMP)9 (cat. no. AF5228) were bought from Affinity Biosciences and primary antibodies against myeloperoxidase (MPO) (cat. no. 22225-1-AP) and β-actin (cat. no. 66009-1-Ig) were purchased from ProteinTech Group, Inc. Secondary anti-rabbit and anti-Mouse IgG (whole molecule)-peroxidase antibody were procured from Sigma-Aldrich Trading Co., Ltd.

Cell culture and drug treatment. The cells were cultured in high-glucose DMEM (cat. no. 2024059) supplemented with 10% FBS (cat. no. 04-001-1A) and 1% Penicillin-Streptomycin solution (cat. no. 2114092) (these were all purchased from Biological Industries) for 24 h in a constant temperature incubator at 37˚C with 5% CO_2, then treated at 37˚C with 10 mM $Na_2S_2O_4$ in the glucose-free medium (cat. no. 2029548; Biological Industries) for 2 h for oxygen and glucose deprivation. Subsequently, the medium was replaced with high-glucose DMEM and reoxygenated at 37˚C for 2 h, which was defined as the oxygen-glucose deprivation/reperfusion model (OGD/R). The cells were randomly divided into Control, OGD/R and drug pretreatment groups. The drug formulation was solubilized in 0.1% DMSO and diluted with DMEM. First, cells were incubated with alexandrine (2.5, 5.0, 10.0, 20.0, 40.0 and 80 μM), para-hydroxybenzaldehyde (2.5, 5.0, 10.0, 20.0, 40.0 and 80.0 μM) and gastrodin (1, 5, 25, 50, 100 and 200 μM) at 37˚C for 24 h. Subsequently, according to the experimental results and previously published protocols (36-38), the pretreatment group was incubated at the same time with the complete DMEM containing 2.5, 5.0 and 10.0 μM para-hydroxybenzaldehyde, 2.5, 5.0 and 10.0 μM alexandrin or 1, 5 and 25 μM gastrodin for subsequent experiments.

Cell viability analysis. Cell viability following treatment was measured by Cell Counting Kit (CCK)-8 assay (Beijing Solarbio Science & Technology Co., Ltd.). Following 2 h reoxygenation, 10 μl CCK-8 solution was added to all groups in a 96-well plate and incubated for 4 h. The optical density (OD) was measured at 450 nm on an enzyme-labeling instrument (Thermo Fisher Scientific, Ltd.). The cell viability rate was calculated as follows: Cell viability rate=[(experimental group OD_{450}-blank OD_{450})/(control group OD_{450}-blank OD_{450})] x100.

Western blot analysis. Cells were treated with Lysis buffer (PSMF:100 mM RIPA, 1:100) (cat. no. 042121210730; 051021210825 Beyotime Biotech Inc) for lysis on ice for 20 min. The lysate was collected by centrifugation at 14,300 x g and 4˚C for 10 min and protein concentration was determined in the supernatant by the BCA method. Total protein (80 μg/lane) was separated by SDS-PAGE on a 6% gel and transferred onto a PVDF membrane. Subsequently, the membrane was blocked with 5% bovine serum albumin at room temperature for 1 h. Membranes were incubated with primary antibody against p-STAT3 (1:1,000), STAT3 (1:1,000), MMP9 (1:1,000), MPO (1:1,000) and β-actin (1:25,000) at 4˚C overnight. Following primary antibody incubation, the membranes were incubated with anti-Rabbit or Anti-Mouse secondary antibody (1:5,000) for 2 h at room temperature. The immunoreactive bands were developed using enhanced chemiluminescence reagent (cat. no. A38555; Thermo Fisher Scientific) and images were captured in the Bio-Rad ChemiDoc™ XRS gel imaging system (Bio-Rad Laboratories, Ltd.). ImageJ Lab™ V4.0 software (Bio-Rad Laboratories, Ltd.) was used to analyzed.

Experimental statistical analysis. GraphPad Prism 9.0.0 software (GraphPad Software, Inc.) was used for statistical analysis. Normal distribution was used Kolmogorov-Smirnov test, and homogeneity of variance was used Brown-Forsythe test. All data conformed to normal distribution and homogeneity of variance. Therefore, multiple comparisons were performed using one-way ANOVA followed by Bonferroni's post hoc test. $P<0.05$ was considered to indicated a statistically significant difference. Data are presented as the mean ± standard error of the mean. Cell viability experiments were repeated 6 times, and western blot experimental was repeated 3 times.

Results

Screening results of active ingredients of GEB. A total of 21 active ingredients of GEB were retrieved from the ETCM database. Subsequently, the 2D structure, molecular formula, and relative molecular weight of each ingredient was obtained from the TCMSP database. The drug-like properties of active ingredients of GEB, including LogD, AlogP, oral bioavailability (OB), drug-likeness (DL), Caco-2 permeability, and BBB transmission, were also obtained (Table I).

Prediction of targets of active ingredients. The targets of the aforementioned 21 active ingredients were predicted using the ETCM and SwissTargetPrediction databases. Notably, only 13 [sitosterol, vanillin, palmitic acid, sucrose, succinic acid, alexandrin, para-hydroxybenzaldehyde, citric acid, protocatechuic aldehyde, bis(4-hydroxybenzyl) ether mono-β-D-glucopyranoside, bis(4-hydroxybenzyl) ether, 4,4'-dihydroxydiphenyl methane and gastrodin] active ingredients were able to predict targets in the aforementioned databases. Following de-duplication, 245 potential targets of GEB were retrieved from the ETCM database (Table SI). Moreover, 571 potential targets were obtained from SwissTargetPrediction database (Table SII). Finally, the potential targets were obtained by merging the two databases and de-duplicated to obtain the unique results, resulting in 752 targets for the active ingredient of GEB (Table SIII).

Identification of IS-associated genes targeted by GEB. Using IS as the keyword, 3,855, 1,159, 10, 106 and 15 IS targets were retrieved from GeneCards (Table SIV), DisGeNET (Table SV), DrugBank (Table SVI), OMIM (Table SVII) and TTD (Table SVIII) databases, respectively. A total of 4,158 potentially disease-associated genes were obtained by combined analysis (de-duplication to retain unique results; Table SIX).

In addition, 476 IS-associated DEGs between 39 IS samples and 24 healthy control subjects were identified based on GSE16561 dataset. Of these, 364 genes were upregulated in IS and 112 were downregulated in IS samples (Fig. S2; Table SX).

Venn analysis of 752 targets of GEB active ingredients, 4,158 potential disease-associated genes and 476 IS-associated DEGs yielded 32 key genes for GEB in treating IS (Fig. 2A; Table SXI). Heat map demonstrated the expression patterns of the 32 key genes between patients with IS and healthy control subjects in the GSE16561 dataset (Fig. 2B).

Functional annotation of key genes. To explore the biological functions of key genes, GO analysis was performed (Table SXII). In the BP category, 'response to oxidative stress', 'neutrophil degranulation' and 'neutrophil activation involved in immune response' were the three most enriched terms (Fig. 3A) and also involved most key genes (all counts, 10).

Table I. Chemical profiling and corresponding candidate target gene.

Chemical	Molecular formula	Molecular weight	ALogP	LogD	2D structure	OB %	Caco-2	BBB	DL
Sitosterol	$C_{29}H_{50}O$	414.71	8.08	8.08	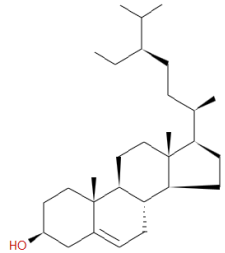	36.91	1.32	0.87	0.75
Vanillin	$C_8H_8O_3$	152.15	1.33	1.06	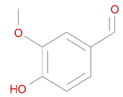	52.00	0.68	0.41	0.03
Palmitic acid	$C_{16}H_{32}O_2$	256.42	6.39	4.94	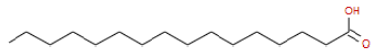	19.30	1.09	1.00	0.10
Sucrose	$C_{12}H_{22}O_{11}$	342.30	-4.31	-4.31	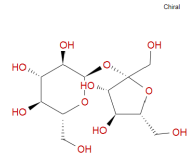	7.17	-2.89	-6.67	0.23
Succinic acid	$C_4H_6O_4$	118.09	-0.36	-3.03	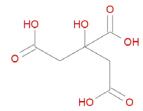	29.62	-0.44	-0.71	0.01
Alexandrin	$C_{35}H_{60}O_6$	576.85	6.34	6.34	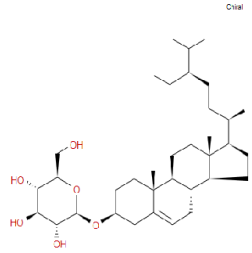	20.46	0.27	-0.27	0.65
P-hydroxybenzaldehyde	$C_7H_6O_2$	122.12	1.35	1.20	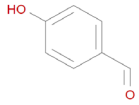	29.98	0.82	0.63	0.02

Table I. Continued.

Chemical	Molecular formula	Molecular weight	ALogP	LogD	2D structure	OB %	Caco-2	BBB	DL
Citric acid	$C_6H_8O_7$	192.12	-1.32	-3.85	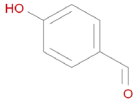	56.22	-1.11	-1.38	0.05
Bis(4-hydroxybenzyl)ether	$C_{14}H_{14}O_3$	230.26	2.73	2.73	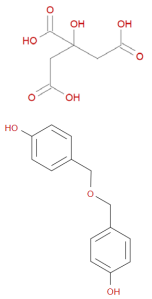				
Protocatechuic aldehyde	$C_7H_6O_3$	138.12	1.11	0.92	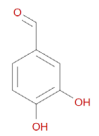	38.35	0.43	0.21	0.03
Bis(4-hydroxybenzyl)ether Mono-Î'-D-glucopyranoside	$C_{20}H_{24}O_8$	392.40	0.80	0.80	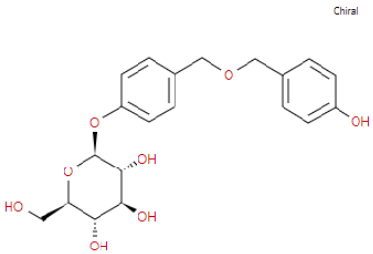				
4,4'-Dihydroxydiphenyl methane	$C_{13}H_{12}O_2$	200.23	3.32	3.32	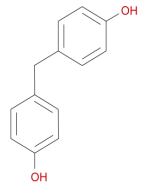				
4-Ethoxymethylphenyl-4'-Hydroxybenzylether	$C_{16}H_{18}O_3$	258.31	3.31	3.31	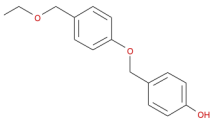				

Table I. Continued.

Chemical	Molecular formula	Molecular weight	ALogP	LogD	2D structure	OB %	Caco-2	BBB	DL
Gastrodamine	$C_{14}H_{15}NO_3$	245.27	2.41	2.66	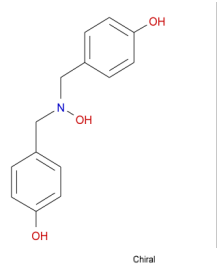				
Gastrodin	$C_{13}H_{18}O_7$	286.28	-0.95	-0.95	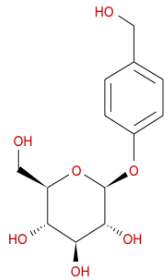	8.19	-1.33	-2.29	0.17
4-Hydroxybenzyl alcohol	$C_7H_8O_2$	124.14	0.98	0.98	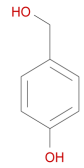	55.19	0.61	0.34	0.02
P-hydroxybenzyl ethyl ether	$C_9H_{12}O_2$	152.19	1.74	1.74	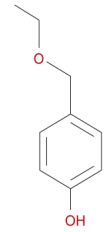				
4-Hydroxybenzyl methyl ether	$C_8H_{10}O_2$	138.16	1.39	1.39	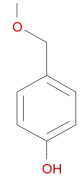				

Table I. Continued.

Chemical	Molecular formula	Molecular weight	ALogP	LogD	2D structure	OB %	Caco-2	BBB	DL
4-(4'-Hydroxybenzyloxy)benzyl methyl ether	$C_{15}H_{16}O_3$	244.29	2.96	2.96	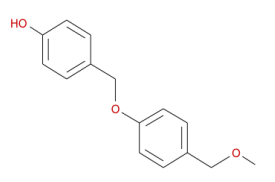				
Tris-[4-(β-D-glucopyranosyloxy) benzyl]citrate	$C_{45}H_{56}O_{25}$	996.91	-2.41	-2.41	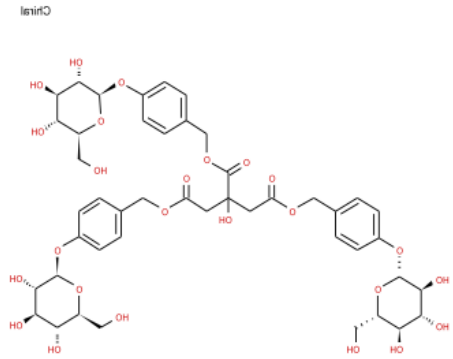				
Vanillyl alcohol	$C_8H_{10}O_3$	154.16	0.97	0.97	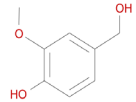				

ALogP, Ghose-Crippen LogKow; LogD, water-octanol distribution coefficient; OB, oral bioavailability; BBB, blood-brain barrier; DL, drug-likeness.

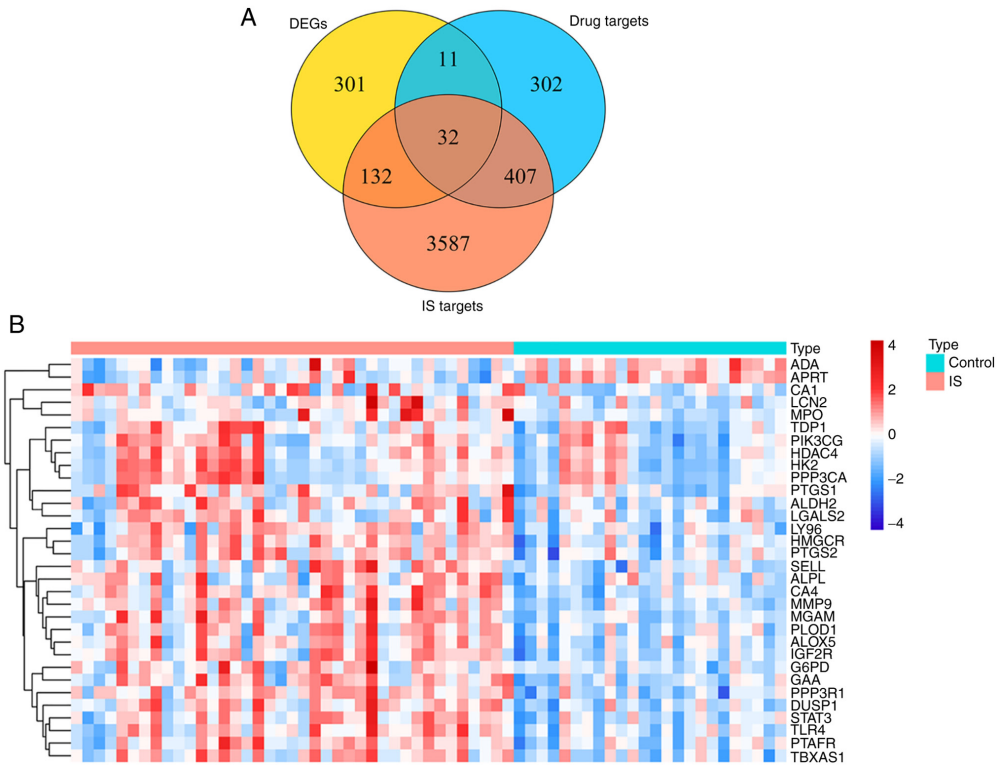

Figure 2. Identification of IS-associated genes targeted by GEB. (A) Venn diagram of intersection of drug and disease targets and DEGs. (B) Expression heat map of key target genes between IS and normal samples. Each square represents a gene. The greater the expression, the darker the color (red, upregulated; blue, downregulated expression). Each row represents the expression of each gene in different samples; column represents expression of all genes in each sample. IS, ischemic stroke; GEB, *Gastrodia elata* Blume; DEG, differentially expressed gene; ADA, adenosine deaminase; APRT, adenine phosphoribosyltransferase; CA1, carbonic anhydrase 1; LCN2, lipocalin 2; MPO, myeloperoxidase; TDP1, tyrosyl-DNA phosphodiesterase 1; PIK3CG, phosphatidylinositol-4,5-bisphosphate 3-kinase catalytic subunit γ; HDAC4, histone deacetylase 4; HK2, hexokinase 2; PPP3CA, protein phosphatase 3 catalytic subunit α; PTGS1, prostaglandin-endoperoxide synthase 1; ALDH2, aldehyde dehydrogenase 1 family member 2; LGALS2, galectin 2; LY96, lymphocyte antigen 96; HMGCR, 3-hydroxy-3-methyl-glutaryl-coenzyme A reductase; PTGS1, prostaglandin-endoperoxide synthase 2: SELL, selectin L; ALPL, alkaline phosphatase, biomineralization associated; CA4, carbonic anhydrase 4; MGAM, maltase-glucoamylase; PLOD1, procollagen-lysine, 2-oxoglutarate 5-dioxygenase; ALOX5, arachidonate 5-lipoxygenase; IGFR2, insulin-like growth factor II receptor; G6PD, glucose-6-phosphate dehydrogenase; GAA, α glucosidase; PPP3R1, protein phosphatase 2B regulatory subunit 1; DUSP1, dual specificity phosphatase 1; TLR4, toll-like receptor 4; PTAFR, platelet activating factor receptor; TBXAS1, thromboxane A synthase 1.

These key genes were also associated with 'regulation of blood circulation' (count, 6). A total of nine entries in the CC category were enriched, with 'secretory granule membrane' the most significant and the term with the most key genes involved (count, 6; Fig. 3B). Among the 30 MF category terms that were significantly enriched, 'carbohydrate binding' was significant (count, 8; Fig. 3C). KEGG analysis suggested that eleven pathways were associated with key genes (Fig. 3D). 'Toxoplasmosis', 'arachidonic acid metabolism', 'lipid and atherosclerosis', 'galactose metabolism' and 'PD-L1 expression and PD-1 checkpoint pathway in cancer' were the top five KEGG pathways (Table SXIII).

Construction and analysis of herb-compound-targets-disease network. Based on the aforementioned results, the active ingredients of GEB and 32 key genes were matched. A herb-compound-target-disease network was constructed, which consisted of 48 nodes (IS, one herb, 14 active compounds and 32 target genes) and 234 edges (Fig. 4A).

Subsequently, all 32 key genes were uploaded into STRING to construct the PPI network. At a confidence level of 0.4, discrete proteins were hidden to obtain a PPI network consisting of 26 genes with 52 edges (Fig. 4B; Table SXIV). The degree value of each gene was calculated using the CytoNCA plugin; toll-like receptor 4 (TLR4), STAT3, MPO, PTGS2 and MMP9 were the top five genes in terms of degree value (Fig. 4C; Table SXV) and were selected as core genes for downstream analysis.

Molecular docking of core genes. TLR4, STAT3, MPO, PTGS2 and MMP9 may be core potential targets of GEB for treating IS. Therefore, the active components and five core gene targets were matched and the docking potential was examined. The binding energy for all compounds and core genes was in the range of -8.2~-4.4 kcal/mol; the larger the absolute value of binding energy, the stronger the molecular docking effect (30,39). Only three core genes, STAT3, MPO and MMP9 had binding energy >-5 kcal/mol with active components of GEB and showed good docking activity (Table II). The present results suggested that the compounds in GEB interacted with core genes to counteract IS.

Molecular docking illustrated the interaction between core genes and compounds; all five compounds interacted with the corresponding targets, primarily via hydrogen bonds. Specifically, palmitic acid formed three hydrogen bonds, primarily with residues LEU-119, PHE-122 and PRO-145 on

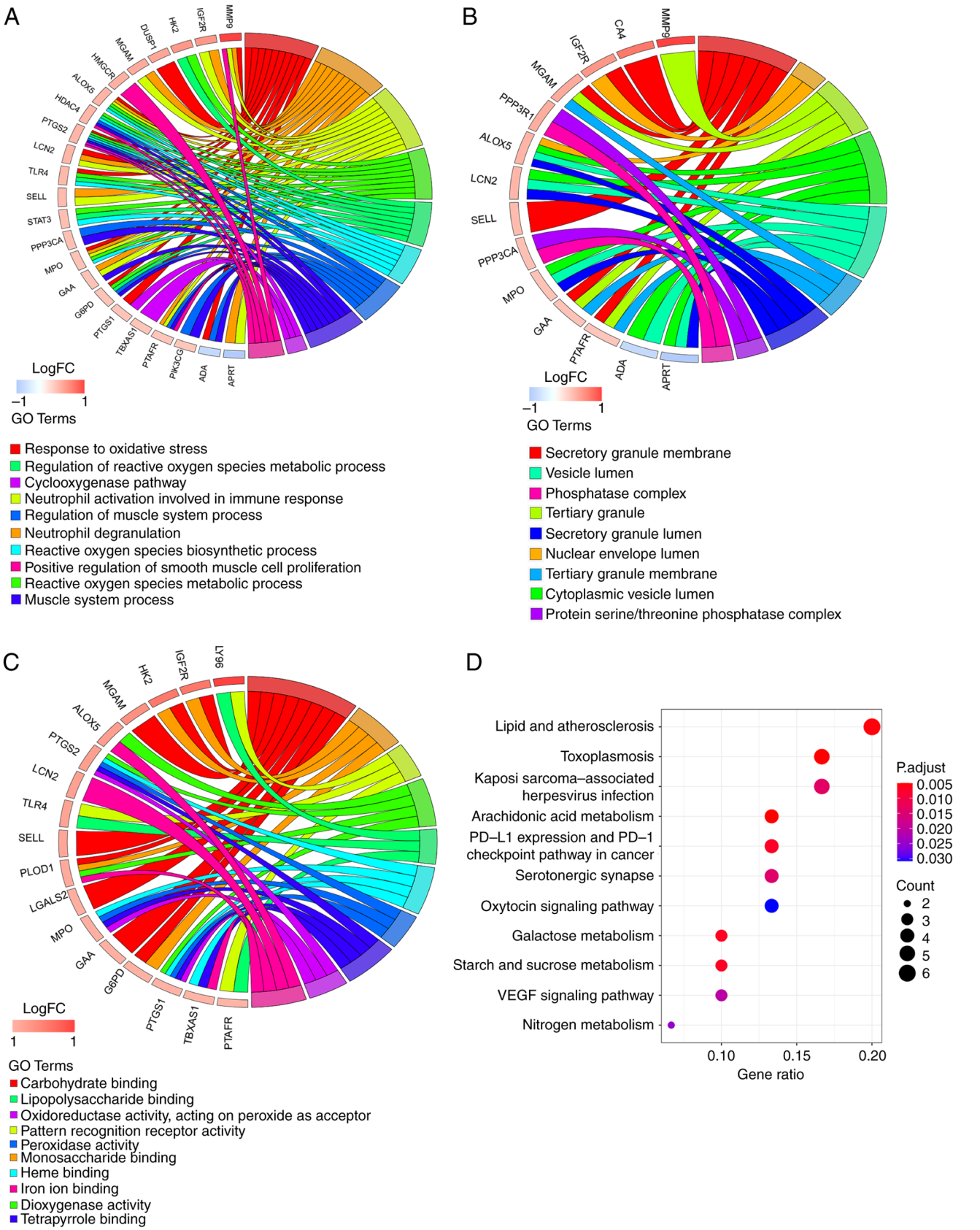

Figure 3. Functional enrichment analysis of 32 key genes. GOChord plot of the association between selected genes and corresponding (A) biological process, (B) cellular component and (C) molecular function terms, with the logFC of the genes. Left, gene regulation; right, GO terms. A gene was linked to a specific GO term by the colored bands. (D) Dot plot of enriched pathways in 32 key genes. The color intensity, enrichment degree of KEGG pathways. Gene ratio, proportion of differential genes in the whole gene set. KEGG, Kyoto Encyclopedia of Genes and Genomes; GO, Gene Ontology; LCN2, lipocalin 2; MPO, myeloperoxidase; HK2, hexokinase 2; PTGS1, prostaglandin-endoperoxide synthase 1; LGALS2, galectin 2; LY96, lymphocyte antigen 96; PTGS1, prostaglandin-endoperoxide synthase 2: SELL, selectin L; MGAM, maltase-glucoamylase; PLOD1, procollagen-lysine, 2-oxoglutarate 5-dioxygenase; ALOX5, arachidonate 5-lipoxygenase; IGFR2, insulin-like growth factor II receptor; G6PD, glucose-6-phosphate dehydrogenase; GAA, α glucosidase; TLR4, toll-like receptor 4; PTAFR, platelet activating factor receptor; TBXAS1, thromboxane A synthase 1; FC, fold change.

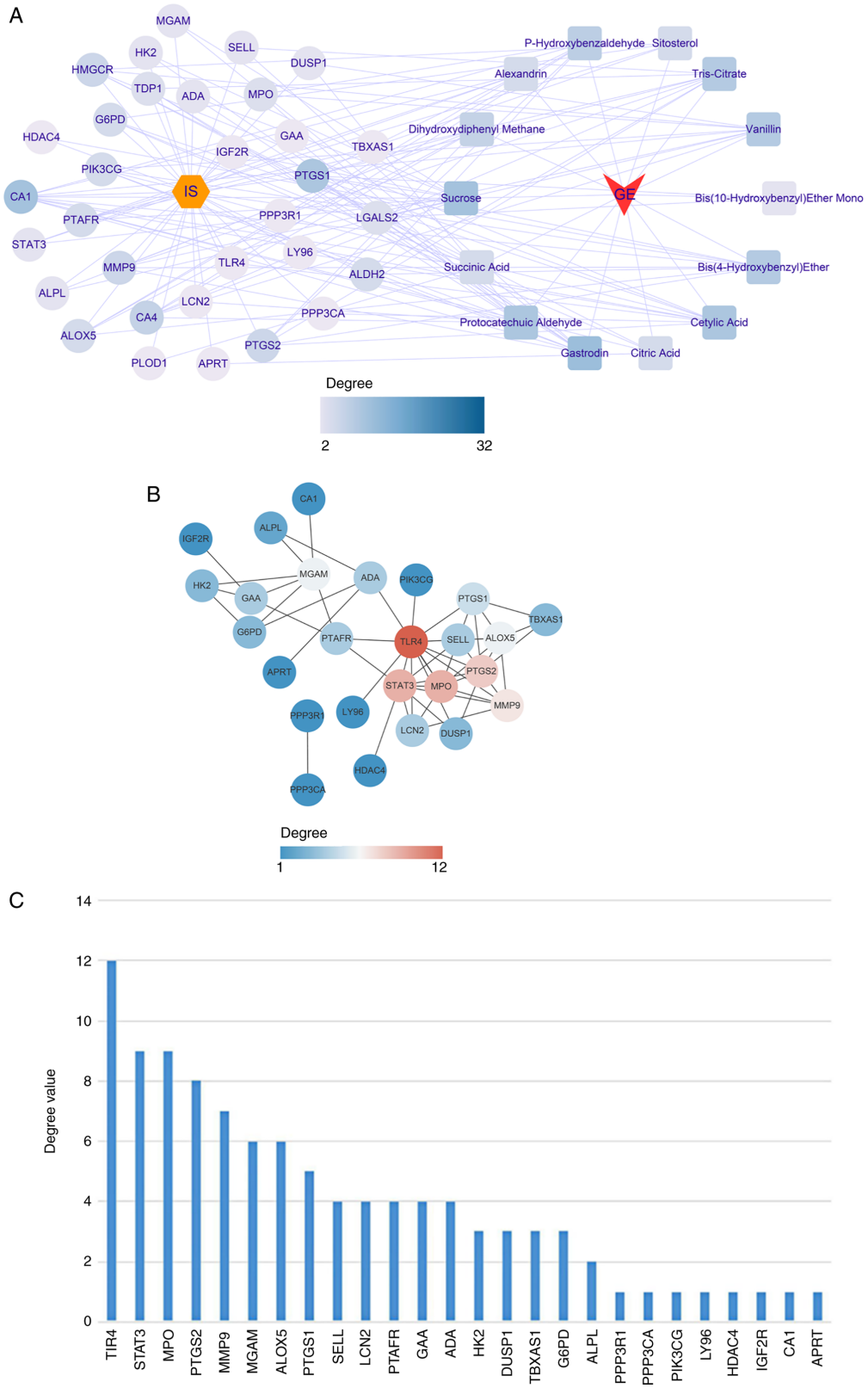

Figure 4. Herb-compound-target-disease network. (A) Correspondence between drugs, active ingredients and key target genes. Yellow hexagon, disease; circle, key target; square, active ingredient of GEB. (B) Protein interaction network of key targets. The lines represent interaction; thickness represents combined degree (combined score). The depth of the color means the degree value, and the higher the degree value, the more the core position. (C) Degree ranking of key targets. GEB, *Gastrodia elata* Blume; ADA, adenosine deaminase; APRT, adenine phosphoribosyltransferase; CA1, carbonic anhydrase 1; LCN2, lipocalin 2; MPO, myeloperoxidase; TDP1, tyrosyl-DNA phosphodiesterase 1; PIK3CG, phosphatidylinositol-4,5-bisphosphate 3-kinase catalytic subunit γ; HDAC4, histone deacetylase 4; HK2, hexokinase 2; PPP3CA, protein phosphatase 3 catalytic subunit α; PTGS1, prostaglandin-endoperoxide synthase 1; ALDH2, aldehyde dehydrogenase 1 family member 2; LGALS2, galectin 2; LY96, lymphocyte antigen 96; HMGCR, 3-hydroxy-3-methyl-glutaryl-coenzyme A reductase; PTGS1, prostaglandin-endoperoxide synthase 2: SELL, selectin L; ALPL, alkaline phosphatase, biomineralization associated; CA4, carbonic anhydrase 4; MGAM, maltase-glucoamylase; PLOD1, procollagen-lysine, 2-oxoglutarate 5-dioxygenase; ALOX5, arachidonate 5-lipoxygenase; IGFR2, insulin-like growth factor II receptor; G6PD, glucose-6-phosphate dehydrogenase; GAA, α glucosidase; PPP3R1, protein phosphatase 2B regulatory subunit 1; DUSP1, dual specificity phosphatase 1; TLR4, toll-like receptor 4; PTAFR, platelet activating factor receptor; TBXAS1, thromboxane A synthase 1.

Table II. Components docked with key targets.

Compounds	Target gene (PDB ID)	Binding energy, kcal/mol
Palmitic acid	TLRA (2Z62), PGTS2 (1PXX)	-4.4
Alexandrin	STAT3 (4ZIA)	-8.2
P-hydroxybenzaldehyde	MPO (6AZP)	-5.4
Gastrodin	MMP9 (5TH6)	-6.8

PDB, protein data bank; TLRA, toll-like receptor 4; PGTS2, prostaglandin-endoperoxide synthase 2; MPO, myeloperoxidase; MMP, matrix metalloproteinase.

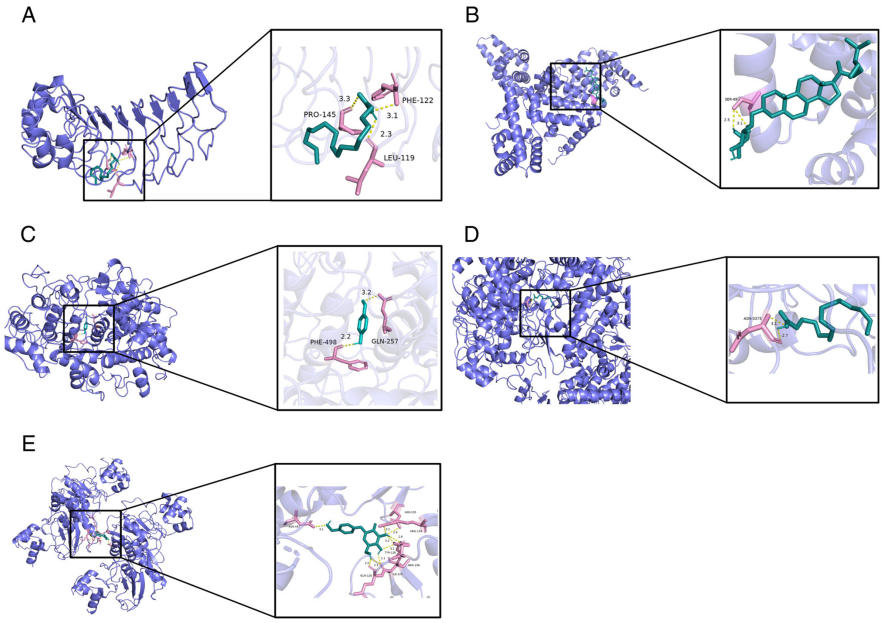

Figure 5. Molecular docking of core genes. Green, active molecules palmitic acid, alexandrin, para-hydroxybenzaldehyde and gastrodin; pink, amino acid residue which has the hydrogen bond interaction with the active component; yellow dotted line, hydrogen bond. (A) TLR4 interaction with palmitic acid. (B) STAT3 interaction with alexandrin. (C) MPO interaction with para-hydroxybenzaldehyde. (D) PTGS2 interaction with palmitic acid. (E) MMP9 interaction with gastrodin. MPO, myeloperoxidase; PTGS2, prostaglandin-endoperoxide synthase 2; TLR4, toll-like receptor 4; MMP, matrix metalloproteinase.

the TLR4 protein (Fig. 5A). SER-69 residue on STAT3 protein was bound to alexandrin through one hydrogen bond (Fig. 5B). Para-hydroxybenzaldehyde formed two hydrogen bonds with two residues (GLN-257 and PHE-498) on the MPO protein (Fig. 5C). Palmitic acid formed two hydrogen bonds with residue HIS-3375 on the PTGS2 protein (Fig. 5D). Finally, gastrodin was bound to the MMP9 protein by nine hydrogen bonds (Fig. 5E).

Viability of HT22 cells following treatment with alexandrin, para-hydroxybenzaldehyde and gastrodin. The present results indicated that gastrodin (1, 5 and 25 μM) did not cause notable cytotoxicity. At concentrations of gastrodin ≥50 μM, cell viability significantly decreased (Fig. 6A). In addition, para-hydroxybenzaldehyde and alexandrin did not affect viability of HT22 cells (Fig. 6B and C). OGD/R significantly decreased viability of HT22 cells. Compared with the OGD/R group, the gastrodin 1 μM group improved cell viability, although not significantly. The para-hydroxybenzaldehyde 2.5 μM group and gastrodin 5.0 μM group increased cell viability increased. Conversely, the gastrodin 25 μM and para-hydroxybenzaldehyde 5 and 10 μM groups increased cell viability significantly (Fig. 6D and E). The cell viability was significantly increased in the 2.5, 5.0 and 10.0 μM groups of alexandrin (Fig. 6F). Thus, it may be speculated that para-hydroxybenzaldehyde, gastrodin and alexandrin promoted viability of HT22 cells.

Western blot analysis. Based on network pharmacology and molecular docking results, western blotting analysis was performed to confirm the regulatory effects of the three active components of GEB, namely alexandrin, para-hydroxybenzaldehyde and gastrodin, on expression of STAT3, MPO and MMP9, which are the core targets, in HT22 cells. The present results showed that compared with the control, the OGD/R group did not show any significant change in the expression of p-STAT3 protein (Fig. 7A) but upregulated protein expression of MPO and MMP9 (Fig. 7B and C). However, expression of p-STAT3 in the alexandrin group was significantly upregulated compared with that in the OGD/R group (Fig. 7A), while total protein expression of STAT3 remained unchanged. MPO expression in the para-hydroxybenzaldehyde group was

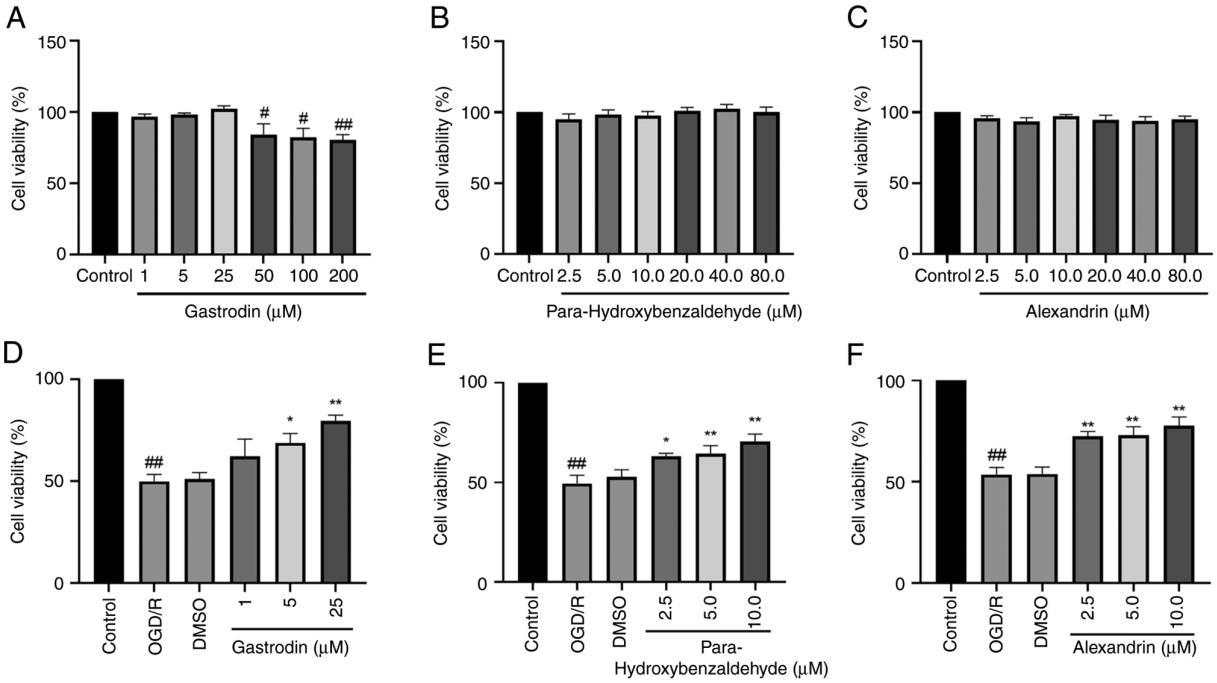

Figure 6. Effect of three GEB active components on viability of HT22 cells. Effect of (A) gastrodin, (B) para-hydroxybenzaldehyde and (C) alexandrin on the viability of HT-22 cells. Cell viability following OGD/R and treatment with (D) gastrodin, (E) para-hydroxybenzaldehyde, (F) alexandrin. $^{\#}$P<0.05 and $^{\#\#}$P<0.01 vs. control. *P<0.05 and **P<0.01 vs. OGD/R. Data are presented as the mean ± standard error of the mean (n=6). GEB, *Gastrodia elata* Blume; OGD/R, oxygen-glucose deprivation-reperfusion.

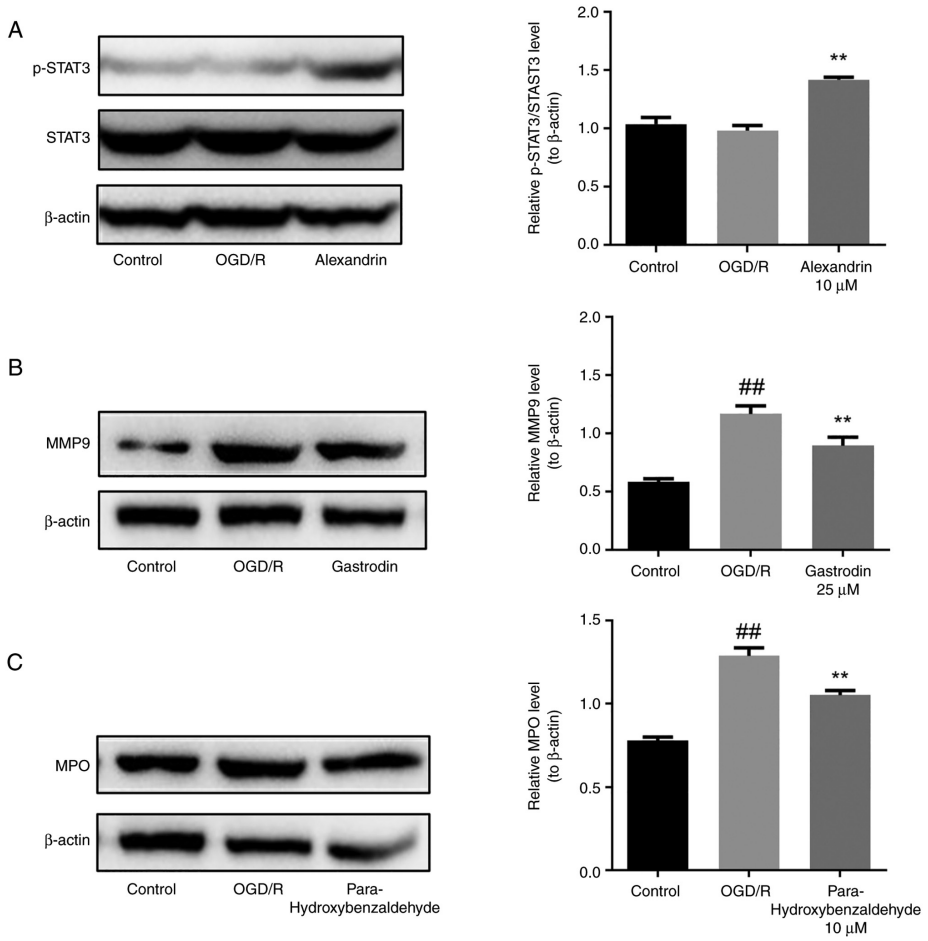

Figure 7. Regulatory effect of three active components of GEB on the core targets in HT22 cells. (A) p-STAT3/STAT3, (B) MPO, (C) MMP9 expression. $^{\#\#}$P<0.01 vs. control; **P<0.01 vs. OGD/R. Data are presented as the mean ± standard error of the mean (n=3). GEB, *Gastrodia elata* Blume; OGD/R, oxygen-glucose deprivation-reperfusion; MPO, myeloperoxidase; p-, phosphorylated; MMP, matrix metalloproteinase.

significantly lower than that in the OGD/R group (Fig. 7B). Moreover, the expression of MMP9 was significantly lower in the gastrodin group than in the OGD/R group (Fig. 7C).

Discussion

GEB protects the BBB by counteracting oxidative stress, decreasing neuroinflammation and inhibiting apoptosis, thereby showing promising neuroprotective properties in the acute phase of cerebral ischemia (40,41). However, as the pathophysiological mechanisms of IS are complex and the active components of GEB are not known, the underlying mechanisms that induce neuroprotection remain unclear (42). Network pharmacology can explore the association between health and IS at the molecular level, as well as the potential mechanism underlying network regulation. Particularly for complex systemic disease, simultaneous multitarget intervention may have a better efficacy and fewer side effects compared with single drug treatment (43). Therefore, in the present study, the GEO database was used in combination with PPI and GO results to improve the accuracy of target prediction. The core targets were enriched in 'atherosclerosis', 'lipid metabolism disorders', and 'AA metabolism'.

A previous study confirmed that 'lipid and atherosclerosis' is one of the main factors in the increase of stroke-related mortality caused by the accumulation of lipids derived from low-density lipoprotein in the arterial wall (44). Pro-inflammatory cytokines (TNF-α and IL-1) and vascular inflammation-associated secreted phospholipases (phospholipase A_2IIA and lipoprotein-associated phospholipase A_2) jointly promote atherosclerotic plaque formation and blood clot release, thereby inducing IS (45,46). At 1 h after the onset of IS, uncontrolled oxidative metabolism of AA pathway results in platelet aggregation and transformation into prostaglandins, which mediates inflammation (47). Following cerebral ischemia, brain tissue necrosis occurs in the ischemic area due to energy store depletion and inflammatory mediators are released to activate the immune response, promoting further release of inflammatory factors (48). PD-1/PD-L1 pathway is involved in maintaining peripheral blood T lymphocyte tolerance and regulating inflammation (49). Also, AKT phosphorylation is inhibited by blocking CD28-mediated phosphatidylinositol 3-kinase (PI3K) activation and preventing inflammatory damage caused by T cell overactivation (50).

Based on KEGG analysis, the genes or proteins involved in the 'atherosclerosis', 'lipid metabolism disorders', and 'AA metabolism' pathway of IS were considered core targets. A total of five genes was identified from the PPI network of 32 key targets, namely TLR4, STAT3, MPO, PTGS2 and MMP9, which may play a key role in the pharmacological function of GEB. Concurrently, following docking of GEB with the five core targets molecule, four potentially active components were obtained: Palmitic acid, alexandrin, para-hydroxybenzaldehyde and gastrodin. Among these, the three active components of GEB, alexandrin, para-hydroxybenzaldehyde and gastrodin, were associated with damage and repair I/R.

Alexandrin is a sterol that promotes proliferation of neural stem cells (36). In a neuronal OGD/R model, it exerts an anti-apoptotic role by activating the AKT signaling pathway (51). A previous study demonstrated that reactivating JAK2/STAT3 signal transduction via the PI3K/AKT pathway inhibits oxidative stress and mitochondrial dysfunction, exerts an anti-apoptosis effect and protects nerve cells (52). Transcription factor STAT3 is a downstream mediator of ATK associated with classical inflammatory disease and is key to the fate of injured nerve cells (53). Therefore, it was speculated that alexandrin activates signal transduction of STAT3 via the PI3K/AKT pathway to initiate anti-inflammation and anti-apoptosis effects and exert neuroprotection after cerebral I/R injury (CIRI). Consistent with the proposed hypothesis, the present results showed that alexandrin elevated expression of p-STAT3 in OGD/R-treated HT22 cells and increased nerve cell viability. Thus, alexandrin may activate STAT3 to serve an anti-CIRI effect. As an efficient and inexpensive neuroprotective agent, alexandrin is expected to be developed as a drug for treating IS (51).

A previous study demonstrated that MPO activity can be used to evaluate the degree of inflammation in ischemic brain tissue (54). Moreover, MPO-induced inflammatory factors activate MMPs, destroy the integrity of BBB and aggravate brain damage (55). Para-hydroxybenzaldehyde is a component of GEB that is considered to protect the brain against CIRI, preserve BBB function and decrease injury following nerve inflammation (56,57). Consistent with previous studies (54,57), our results showed that para-hydroxybenzaldehyde protects HT22 cells from OGD/R-induced damage by inhibiting the activity of MPO. This finding suggested that the neuroprotective effect of para-hydroxybenzaldehyde on IS is associated with its anti-inflammatory properties.

Gastrodin is a phenolic glycoside and the primary bioactive component of GE (58). Moreover, gastrodin content is the most critical marker in the quality control of GE (59). Gastrodin has anti-CIRI effects and is used to treat central nervous system disease (60). Both *in vivo* and *in vitro* studies have confirmed that pretreatment with gastrodin significantly decreases expression of inflammatory cytokine MMP9, thus protecting the integrity of the basement membrane in brain endothelial cells, reversing the damage to the BBB and decreasing the inflammatory response of I/R (61,62). Similarly, the present study showed that gastrodin increased cell viability in a dose-dependent manner and decreased expression of MMP9 in the OGD/R group. Therefore, it was speculated that gastrodin decreased cell inflammation by inhibiting the activity of MMP9 following CIRI, repairing BBB, and playing an anti-IS role. In addition, gastrodin also improves neurological function and decreases brain injury before and after surgery (63). Moreover, it exerts a neuroprotective effect after 7 days of reperfusion (64), indicating a lasting role during IS treatment.

In summary, the present study investigated the potential mechanism of GEB in IS based on network pharmacology. Different from the traditional enrichment analysis method (65), the present study identified DEGs to analysis of genes with significant differences in expression between patients with IS and healthy control subjects. The present results indicated that TLR4, STAT3, MPO, PTGS2 and MMP9 were primarily associated with inflammation and apoptosis. Furthermore, the primary pathways of key targets of GEB were associated with inflammation, including 'AA metabolism', 'lipid and atherosclerosis' and 'PD-1/PD-L1 pathway'. Moreover, improving IS by GEB may regulate inflammatory immune response and

protect the BBB by interfering with key targets. According to the present molecular docking and *in vitro* results, the three active components of GEB stably bound to the three core targets and exerted a neuroprotective role against CIRI by regulating these core targets. Therefore, it was speculated that alexandrin, the active component of GE, may significantly promote expression of STAT3 and be involved in anti-inflammation and anti-apoptosis effects. On the other hand, para-hydroxybenzaldehyde and gastrodin downregulated expression of MPO and MMP9, respectively, inhibiting the inflammatory response and BBB damage to protect ischemic neurons, thereby exerting an anti-CIRI role. The present results provided a novel theoretical basis for the clinical application of GEB in the treatment of IS. However, in-depth experimental verification of the mechanism of action is needed.

Acknowledgements

Not applicable.

Funding

The present study was supported by the National Natural Science Foundation of China (grant no. 81960733), the Applied Basic Research Program of Yunnan Province (grant no. 2019FB120) and the Scientific Research Foundation of The Education Department of Yunnan Province (grant no. 2022Y337).

Availability of data and materials

The datasets used and/or analyzed during the current study are available from the corresponding author on reasonable request.

Authors' contributions

XD and LY conceived and designed this study. YL and LY participated in the experiments. PC and YL analyzed the data. YL wrote the manuscript. All authors have read and approved the final manuscript. YL and XD confirm the authenticity of all the raw data.

Ethics approval and consent to participate

Not applicable.

Patient consent for publication

Not applicable.

Competing interests

The authors declare that they have no competing interests.

References

1. Kuklina EV, Tong X, George MG and Bansil P: Epidemiology and prevention of stroke: A worldwide perspective. Expert Rev Neurother 12: 199-208, 2012.
2. GBD 2016 Neurology Collaborators: Global, regional, and national burden of neurological disorders, 1990-2016: A systematic analysis for the global burden of disease study 2016. Lancet Neurol 18: 459-480, 2019.
3. Mendelson SJ and Prabhakaran S: Diagnosis and management of transient ischemic attack and acute ischemic stroke: A review. JAMA 325: 1088-1098, 2021.
4. Paul S and Candelario-Jalil E: Emerging neuroprotective strategies for the treatment of ischemic stroke: An overview of clinical and preclinical studies. Exp Neurol 335: 113518, 2021.
5. Zhang C, Liao Y, Liu L, Sun Y, Lin S, Lan J, Mao H, Chen H and Zhao Y: A network pharmacology approach to investigate the active compounds and mechanisms of musk for ischemic stroke. Evid Based Complement Alternat Med 2020: 4063180, 2020.
6. Chavez LM, Huang SS, MacDonald I, Lin JG, Lee YC and Chen YH: Mechanisms of acupuncture therapy in ischemic stroke rehabilitation: A literature review of basic studies. Int J Mol Sci 18: 2270, 2017.
7. Venketasubramanian N: Complementary and alternative interventions for stroke recovery-a narrative overview of the published evidence. J Complement Integr Med 18: 553-559, 2021.
8. Han SY, Hong ZY, Xie YH, Zhao Y and Xu X: Therapeutic effect of Chinese herbal medicines for post stroke recovery: A traditional and network meta-analysis. Medicine (Baltimore) 96: e8830, 2017.
9. Hsieh CL, Chiang SY, Cheng KS, Lin YH, Tang NY, Lee CJ, Pon CZ and Hsieh CT: Anticonvulsive and free radical scavenging activities of *Gastrodia elata* Bl. in kainic acid-treated rats. Am J Chin Med 29: 331-341, 2001.
10. Zhu H, Liu C, Hou J, Long H, Wang B, Guo D, Lei M and Wu W: *Gastrodia elata* Blume polysaccharides: A review of their acquisition, analysis, modification, and pharmacological activities. Molecules 24: 2436, 2019.
11. Wang ZH, Chen BH, Lin YY, Xing J, Wei ZL and Ren L: Herbal decoction of Gastrodia, Uncaria, and Curcuma confers neuroprotection against cerebral ischemia in vitro and in vivo. J Integr Neurosci 19: 513-519, 2020.
12. Xu N, Li M, Wang P, Wang S and Shi H: Spectrum-effect relationship between antioxidant and anti-inflammatory effects of banxia baizhu tianma decoction: An identification method of active substances with endothelial cell protective effect. Front Pharmacol 13: 823341, 2022.
13. He KL, Zhang P and Liu XL: Tianma injection in the treatment of vertebral basilar artery insufficiency randomized parallel group study. J Pract Tradit Chin Intern Med 28: 44-46, 2014.
14. Tang X, Lu J, Chen H, Zhai L, Zhang Y, Lou H. Wang Y, Sun L and Song B: Underlying mechanism and active ingredients of tianma gouteng acting on cerebral infarction as determined via network pharmacology analysis combined with experimental validation. Front Pharmacol 12: 760503, 2021.
15. Duan X, Wang W, Liu X, Yan H, Dai R and Lin Q: Neuroprotective effect of ethyl acetate extract from *Gastrodia elata* against transient focal cerebral ischemia in rats induced by middle cerebral artery occlusion. J Tradit Chin Med 35: 671-678, 2015.
16. He F, Duan X, Dai R, Wang W, Yang C and Lin Q: Protective effects of Ethyl acetate extraction from *Gastrodia elata* Blume on blood-brain barrier in focal cerebral ischemia reperfusion. Afr J Tradit Complement Altern Med 13: 199-209, 2016.
17. Wang T, Chen H, Xia S, Chen X, Sun H and Xu Z: Ameliorative effect of parishin C against cerebral ischemia-induced brain tissue injury by reducing oxidative stress and inflammatory responses in rat model. Neuropsychiatr Dis Treat 17: 1811-1823, 2021.
18. Ruan Y, Yao L, Zhang B, Zhang S and Guo J: Nanoparticle-mediated delivery of neurotoxin-II to the brain with intranasal administration: An effective strategy to improve antinociceptive activity of neurotoxin. Drug Dev Ind Pharm 38: 123-128, 2012.
19. Nogales C, Mamdouh ZM, List M, Kiel C, Casas AI and Schmidt HHHW: Network pharmacology: Curing causal mechanisms instead of treating symptoms. Trends Pharmacol Sci 43: 136-150, 2022.
20. Zhang R, Zhu X, Bai H and Ning K: Network pharmacology databases for traditional Chinese medicine: Review and assessment. Front Pharmacol 10: 123, 2019.
21. Daina A, Michielin O and Zoete V: SwissTargetPrediction: Updated data and new features for efficient prediction of protein targets of small molecules. Nucleic Acids Res 47 (W1): W357-W364, 2019.
22. Ritchie ME, Phipson B, Wu D, Hu Y, Law CW, Shi W and Smyth GK: limma powers differential expression analyses for RNA-sequencing and microarray studies. Nucleic Acids Res 43: e47, 2015.
23. Yu G, Wang LG, Han Y and He QY: clusterProfiler: An R package for comparing biological themes among gene clusters. OMICS 16: 284-287, 2012.

24. Otasek D, Morris JH, Bouças J, Pico AR and Demchak B: Cytoscape automation: Empowering workflow-based network analysis. Genome Biol 20: 185, 2019.
25. Szklarczyk D, Morris JH, Cook H, Kuhn M, Wyder S, Simonovic M, Santos A, Doncheva NT, Roth A, Bork P, *et al*: The STRING database in 2017: Quality-controlled protein-protein association networks, made broadly accessible. Nucleic Acids Res 45 (D1): D362-D368, 2017.
26. Szklarczyk D, Franceschini A, Wyder S, Forslund K, Heller D, Huerta-Cepas J, Simonovic M, Roth A, Santos A, Tsafou KP, *et al*: STRING v10: Protein-protein interaction networks, integrated over the tree of life. Nucleic Acids Res 43 (Database Issue): D447-D452, 2015.
27. Tang Y, Li M, Wang J, Pan Y and Wu FX: CytoNCA: A cytoscape plugin for centrality analysis and evaluation of protein interaction networks. Biosystems 127: 67-72, 2015.
28. Trott O and Olson AJ: AutoDock Vina: Improving the speed and accuracy of docking with a new scoring function, efficient optimization, and multithreading. J Comput Chem 31: 455-461, 2010.
29. Seeliger D and de Groot BL: Ligand docking and binding site analysis with PyMOL and Autodock/Vina. J Comput Aided Mol Des 24: 417-422, 2010.
30. Liang Y, Liang B, Wu XR, Chen W and Zhao LZ: Network pharmacology-based systematic analysis of molecular mechanisms of dingji fumai decoction for ventricular arrhythmia. Evid Based Complement Alternat Med 2021: 5535480, 2021.
31. Morris GM, Huey R and Olson AJ: Using AutoDock for ligand-receptor docking. Curr Protoc Bioinformatics Chapter 8: Unit 8.14, 2008.
32. Yang Y, He Y, Wei X, Wan H, Ding Z, Yang J and Zhou H: Network pharmacology and molecular docking-based mechanism study to reveal the protective effect of salvianolic acid C in a rat model of ischemic stroke. Front Pharmacol 12: 799448, 2022.
33. Ito K and Murphy D: Application of ggplot2 to pharmacometric graphics. CPT Pharmacometrics Syst Pharmacol 2: e79, 2013.
34. Le TT and Moore JH: treeheatr: An R package for interpretable decision tree visualizations. Bioinformatics 37: 282-284, 2021.
35. Walter W, Sanchez-Cabo F and Ricote M: GOplot: An R package for visually combining expression data with functional analysis. Bioinformatics 31: 2912-2914, 2015.
36. Jiang LH, Yang NY, Yuan XL, Zou YJ, Zhao FM, Chen JP, Wang MY and Lu DX: Daucosterol promotes the proliferation of neural stem cells. J Steroid Biochem Mol Biol 140: 90-99, 2014.
37. Jiang T, Cheng H, Su J, Wang X, Wang Q, Chu J and Li Q: Gastrodin protects against glutamate-induced ferroptosis in HT-22 cells through Nrf2/HO-1 signaling pathway. Toxicol In Vitro 62: 104715, 2020.
38. Xiang B, Chun X, Shen T, Jiang S, Lin Q and Li XF: 4-hydroxybenzyl aldehyde can prevent the acute cerebral ischemic injury in rats. Chin Tradit Pat Med 39: 1572-1576, 2017 (In Chinese).
39. Xiong H, Dong Z, Lou G, Gan Q, Wang J and Huang Q: Analysis of the mechanism of Shufeng Jiedu capsule prevention and treatment for COVID-19 by network pharmacology tools. Eur J Integr Med 40: 101241, 2020.
40. Heese K: *Gastrodia elata* Blume (Tianma): Hope for brain aging and dementia. Evid Based Complement Alternat Med 2020: 8870148, 2020.
41. Xia C, Zhou H, Xu X, Jiang T, Li S, Wang D, Nie Z and Sheng Q: Identification and investigation of miRNAs From *Gastrodia elata* Blume and their potential function. Front Pharmacol 11: 542405, 2020.
42. Jurcau A and Ardelean IA: Molecular pathophysiological mechanisms of ischemia/reperfusion injuries after recanalization therapy for acute ischemic stroke. J Integr Neurosci 20: 727-744, 2021.
43. Wang X, Wang ZY, Zheng JH and Li S: TCM network pharmacology: A new trend towards combining computational, experimental and clinical approaches. Chin J Nat Med 19: 1-11, 2021.
44. Khatana C, Saini NK, Chakrabarti S, Saini V, Sharma A, Saini RV and Saini AK: Mechanistic insights into the oxidized low-density lipoprotein-induced atherosclerosis. Oxid Med Cell Longev 2020: 5245308, 2020.
45. Chow YL, Teh LK, Chyi LH, Lim LF, Yee CC and Wei LK: Lipid metabolism genes in stroke pathogenesis: The atherosclerosis. Curr Pharm Des 26: 4261-4271, 2020.
46. Adibhatla RM and Hatcher JF: Altered lipid metabolism in brain injury and disorders. Subcell Biochem 49: 241-268, 2008.
47. Wang B, Wu L, Chen J, Dong L, Chen C, Wen Z, Hu J, Fleming I and Wang DW: Metabolism pathways of arachidonic acids: Mechanisms and potential therapeutic targets. Signal Transduct Target Ther 6: 94, 2021.
48. Anrather J and Iadecola C: Inflammation and stroke: An overview. Neurotherapeutics 13: 661-670, 2016.
49. Ai L, Xu A and Xu J: Roles of PD-1/PD-L1 pathway: Signaling, cancer, and beyond. Adv Exp Med Biol 1248: 33-59, 2020.
50. Schütz F, Stefanovic S, Mayer L, von Au A, Domschke C and Sohn C: PD-1/PD-L1 pathway in breast cancer. Oncol Res Treat 40: 294-297, 2017.
51. Jiang LH, Yuan XL, Yang NY, Ren L, Zhao FM, Luo BX, Bian YY, Xu JY, Lu DX, Zheng YY, *et al*: Daucosterol protects neurons against oxygen-glucose deprivation/reperfusion-mediated injury by activating IGF1 signaling pathway. J Steroid Biochem Mol Biol 152: 45-52, 2015.
52. Gao GS, Li Y, Zhai H, Bi JW, Zhang FS, Zhang XY and Fan SH: Humanin analogue, S14G-humanin, has neuroprotective effects against oxygen glucose deprivation/reoxygenation by reactivating Jak2/Stat3 signaling through the PI3K/AKT pathway. Exp Ther Med 14: 3926-3934, 2017.
53. Zhang Z and Yang W: Paeoniflorin protects PC12 cells from oxygen-glucose deprivation/reoxygenation-induced injury via activating JAK2/STAT3 signaling. Exp Ther Med 21: 572, 2021.
54. Lei JR, Tu XK, Wang Y, Tu DW and Shi SS: Resveratrol down-regulates the TLR4 signaling pathway to reduce brain damage in a rat model of focal cerebral ischemia. Exp Ther Med 17: 3215-3221, 2019.
55. Chen S, Chen H, Du Q and Shen J: Targeting myeloperoxidase (MPO) mediated oxidative stress and inflammation for reducing brain ischemia injury: Potential application of natural compounds. Front Physiol 11: 433, 2020.
56. Zhu YP, Li X, Du Y, Zhang L, Ran L and Zhou NN: Protective effect and mechanism of p-hydroxybenzaldehyde on blood-brain barrier. Zhongguo Zhong Yao Za Zhi 43: 1021-1027, 2018 (In Chinese).
57. Chen KY, Chen YJ, Cheng CJ, Jhan KY, Chiu CH and Wang LC: 3-hydroxybenzaldehyde and 4-hydroxybenzaldehyde enhance survival of mouse astrocytes treated with angiostrongylus cantonensis young adults excretory/secretory products. Biomed J 44 (6 Suppl 2): S258-S266, 2021.
58. Jang JH, Son Y, Kang SS, Bae CS, Kim JC, Kim SH, Shin T and Moon C: Neuropharmacological potential of *Gastrodia elata* Blume and its components. Evid Based Complement Alternat Med 2015: 309261, 2015.
59. Tao J, Luo ZY, Msangi CI, Shu XS, Wen L, Liu SP, Zhou CQ, Liu RX and Hu WX: Relationships among genetic makeup, active ingredient content, and place of origin of the medicinal plant Gastrodia tuber. Biochem Genet 47: 8-18, 2009.
60. Liu Y, Gao J, Peng M, Meng H, Ma H, Cai P, Xu Y, Zhao Q and Si G: A review on central nervous system effects of gastrodin. Front Pharmacol 9: 24, 2018.
61. Li S, Bian L, Fu X, Ai Q, Sui Y, Zhang A, Gao H, Zhong L and Lu D: Gastrodin pretreatment alleviates rat brain injury caused by cerebral ischemic-reperfusion. Brain Res 1712: 207-216, 2019.
62. Wang J and Wu M: The up-regulation of miR-21 by gastrodin to promote the angiogenesis ability of human umbilical vein endothelial cells by activating the signaling pathway of PI3K/Akt. Bioengineered 12: 5402-5410, 2021.
63. Zhang ZL, Gao YG, Zang P, Gu PP, Zhao Y, He ZM and Zhu HY: Research progress on mechanism of gastrodin and p-hydroxybenzyl alcohol on central nervous system. Zhongguo Zhong Yao Za Zhi 45: 312-320, 2020 (In Chinese).
64. Peng Z, Wang S, Chen G, Cai M, Liu R, Deng J, Liu J, Zhang T, Tan Q and Hai C: Gastrodin alleviates cerebral ischemic damage in mice by improving anti-oxidant and anti-inflammation activities and inhibiting apoptosis pathway. Neurochem Res 40: 661-673, 2015.
65. Yuan H, Ma Q, Cui H, Liu G, Zhao X, Li W and Piao G: How can synergism of traditional medicines benefit from network pharmacology? Molecules 22: 1135, 2017.